Nanostructure enhanced near-field radiative heat transfer and designs for energy conversion devices

Wang, B.; Lin, C.; Teo, K.H.

TR2017-110   August 2017

Abstract

Near-field radiative heat transfer can exceed the blackbody limit, and this property has been explored toward energy transfer and conversion applications, such as thermophtovoltaic (TPV) devices, radiative cooling devices, and thermoradiative (TR) devices. The coupling of resonant modes between two surfaces is important in near-field heat transfer and near-field TPV and TR systems. It was shown that the coupling of resonant modes enhances the transmissivity between two coupled objects, which further determines the radiative heat transfer and energy conversion. Surface plasmon polaritons (SPPs), which are surface resonances existing on metal surfaces, are commonly used for such systems. While the frequency of SPP resonance is fixed for a planar emitter, a nanostructured emitter supports additional resonances such as SPP or cavity modes with lower frequencies that are closer to the bandgap energy of a typical PV cell. We show that the nanostrctured designs significantly improves the near-field radiative power transfer, and electric power output for a TR system.

SPIE Optics and Photonics

Nanostructure enhanced near-field radiative heat transfer and designs for energy conversion devices

Bingnan Wang[a], Chungwei Lin[a], and Koon Hoo Teo[a]

[a]Mitsubishi Electric Research Laboratories, 201 Broadway Ste 8, Cambridge, MA 02139 USA

ABSTRACT

Near-field radiative heat transfer can exceed the blackbody limit, and this property has been explored toward energy transfer and conversion applications, such as thermophtovoltaic (TPV) devices, radiative cooling devices, and thermoradiative (TR) devices. The coupling of resonant modes between two surfaces is important in near-field heat transfer and near-field TPV and TR systems. It was shown that the coupling of resonant modes enhances the transmissivity between two coupled objects, which further determines the radiative heat transfer and energy conversion. Surface plasmon polaritons (SPPs), which are surface resonances existing on metal surfaces, are commonly used for such systems. While the frequency of SPP resonance is fixed for a planar emitter, a nanostructured emitter supports additional resonances such as SPP or cavity modes with lower frequencies that are closer to the bandgap energy of a typical PV cell. We show that the nanostrctured designs significantly improves the near-field radiative power transfer, and electric power output for a TR system.

1. INTRODUCTION

Near-field radiation is an important heat transfer mechanism that has great potential in many applications, including thermal imaging, sensing, radiative cooling, and energy conversion in thermophotovoltaic (TPV) systems.[1–3] A TPV system converts heat into electricity through thermal radiation,[4–11] and consists of a thermal emitter and a semiconductor photovoltaic (PV) cell. A heat source keeps the thermal emitter at a high temperature, and generates thermal radiation, which is then absorbed by the PV cell with bandgap energy $E_g = \hbar\omega_g$.[6–8] Assuming all photons with energy larger than E_g absorbed by the PV cell generates an electron-hole pair, Carnot efficiency limit can only be reached with monochromatic radiation from the emitter that is matched to E_g.[4,5] However, for a far-field based TPV system, the emission power is limited by the blackbody radiation, and the emissivity cannot exceed unity at any given frequency. Therefore, the emission power from the emitter would be infinitesimally small assuming a monochromatic radiation spectrum. On the other hand, the near-field based radiative heat transfer can exceed the blackbody limit due to the contributions from evanescent modes.[12–15] In particular, when resonant modes are supported by the emitter and/or absorber, and the separation between the emitter and absorber is a fraction of the wavelength determined by the resonant modes, the absorption spectrum has strong peaks at resonant energies with intensity a few orders exceeding the blackbody limit.[13,16] Near-field based TPV systems have been proposed for improving the power density and efficiency by utilizing resonant modes such as surface phonon polaritons and surface plasmon polaritons (SPPs).[17–23]

Recently, thermoradiative (TR) cells have been proposed as heat engines to convert heat into electricity.[24–27] The simplest form of a TR cell consists of a p-n junction that is heated to a higher temperature T_c than ambient T_a. In Ref.,[24] the working principle of the TR cell was proposed, and the fundamental limit of its power conversion efficiency was analyzed using the Shockley-Queisser framework. The concept was demonstrated with experiments,[26] although the realized efficiency was low. Similar to a TPV system, with resonant coupling in the near-field, the radiation can go beyond the blackbody limit, and all the radiation power can be concentrated into a narrow bandwidth around the resonance.[28] Based on this understanding, in Ref.,[27] a heat sink was placed in close vicinity of the TR cell. It was shown that by near-field coupling of the photons generated from the TR cell to the phonon polariton mode that is supported on the surface of the heat sink (whose dispersion is described by a Lorentz model), both the conversion efficiency and the generated power density can be greatly enhanced when the resonance is very close to the bandgap energy of the TR cell. In Ref.,[29] the near-field enhancement effect of TR cells was further explored, and it was shown that a metallic material, whose dispersion is described by a Drude model and supports surface plasmon polaritons (SPPs), is also good candidate for heat sink, and can have even more significant output power density enhancement effect as compared with Lorentz type materials.

An added advantage with metals as heat sink is their typically larger thermal conductivities compared with insulators. The faster heat dissipation makes it easier to maintain a temperature close to the ambient. To use TR cell based devices to harvest low-grade waste heat with temperature of 1000 K or lower, the preferred band gap energy of TR cell is 0.3 eV or lower.[24] In order for the near-field resonant coupling to work, the resonant mode needs to have an energy slightly above the band gap energy of the cell. However, typical noble metals have surface plasmon resonance with much higher energy.[30]

This huge difference can be compensated by adding nanostructures on the heat sink. In particular, we show that periodic grating structure introduces additional surface resonance modes with energies much lower than SPP modes, and are much closer to the band gap energy of the TR cell. Depending on the material and geometrical parameters of the grating, different resonant modes can be utilized, such as localized SPPs, waveguide modes, and spoof polaritons.[31] We show with calculation that enhanced power generation can be achieved from TR devices with nanostructured heat sink.

2. TPV AND TR DEVICES

For a semiconductor diode at temperature T_c exchanging energy via radiation of photons with a thermal reservoir (either a heat source or a heat sink) at temperature T_a, the photon emission and absorption is due to to transitions across the band gap and is associated with electron-hole (e-h) pair recombination and generation, respectively.[4, 24, 29] When $T_c = T_a$, the emitted photon flux from the cell is the same as the photon flux absorbed by it, and the e-h population is in equilibrium determined by T_c, meaning no current can be generated when an external load is connected to the cell. When $T_c \neq T_a$, there will be an imbalance in photon emission and absorption, therefore a splitting of quasi-Fermi levels, $\Delta\mu$, of electrons and holes.

In the case of TR cell, $T_c > T_a$, the emitted photon flux is larger than the absorbed photon flux, and the e-h population becomes smaller than the equilibrium at T_c. As a result, the cell tends to get back to the equilibrium by generating e-h pairs via all possible channels. Because of this tendency, when connected to an external load, the cell will transfer electrons in the valence band to conduction band through the load, effectively generating an electric current. In comparison, a PV cell has $T_c < T_a$, absorbs more photons than emitted, and accumulates more e-h pairs than the equilibrium state, therefore has a tendency to recombine through all possible channels. When connected to an external load, the PV cell transfers electron in the conduction band to valence band through the load, effectively generating a current flow in an opposite direction as the current generated by a TR cell.

More detailed description and analysis of the physical picture, as well as the mathematical model of the TR cell were given in previous papers.[24, 29] The generated current density is given by the elementary charge $q(>0)$ times the net flux of photons absorbed by the cell $\dot{N}(T_c, \Delta\mu; T_a)$.

$$I(\Delta\mu) = q\dot{N}(T_c, \Delta\mu; T_s) = q \int_{\omega_g}^{\infty} \frac{d\omega}{2\pi} \varepsilon_{c,a}(\omega) \left[\Theta(\omega; T_a, 0) - \Theta(\omega; T_c, \Delta\mu)\right], \tag{1}$$

where $\Theta(\omega; T, \mu) = \frac{1}{\exp[(\hbar\omega - \mu)/k_B T] - 1}$ is the generalized Planck distribution of photons at the frequency ω, at a temperature T and a chemical potential μ, with k_B the Boltzmann constant. $\varepsilon_{c,a}(\omega)$ is the transmissivity between the cell and a heat sink. The generated voltage is $V = \Delta\mu/q$. Therefore the output power density to the load can be calculated as $P_l(\Delta\mu) = VI(\Delta\mu) = \Delta\mu \cdot \dot{N}(T_c, \Delta\mu; T_a)$.

Similarly, the net radiation power absorbed by the cell is calculated, and the

$$P_c(T_c, \Delta\mu; T_a) = \int_0^{\infty} \frac{d\omega}{2\pi} \hbar\omega \cdot \varepsilon_{c,a}(\omega) \left[\Theta(\omega; T_a, 0) - \Theta(\omega; T_c, \Delta\mu)\right]. \tag{2}$$

Note that both the net flux of photons $\dot{N}$ and the radiation P_c to the cell are negative, since more photons are emitted. Hence the efficiency of the TR cell, calculated by $\eta_{TR} = P_l/(P_l - P_c)$ is always smaller than one.

From the above analysis and equations 1 and 2, we can see that with given thermodynamic parameters (temperatures T_c and T_a, and chemical potential $\Delta\mu$), the performance of a TR cell depends only on the transmittivity, which is defined as $\varepsilon_{c,a}(\omega) = 2 \times \frac{1}{(2\pi)^2} \int \varepsilon_{c,a}(\omega, \mathbf{K}) d^2\mathbf{K}$, where $\mathbf{K}$ is the in-plane wavevector.

The transmissivity depends on the optical properties of materials and the gemoetrical parameters rather than thermodynamic parameters. When the two objects are far away, only propagating wavevector components $|\mathbf{K}| = k < \omega/c$ contribute to the transmissivity, and the upper bound of radiation power is blackbody limit.

3. NEAR-FIELD ENHANCED DEVICES

When the distance between the two objects is smaller than the photon wavelength, evanescent wavevector components also contributes to the transmissivity due to photon tunneling.[12] Furthermore, when surface resonances are supported in the system, strong resonant coupling in the near-field can reshape the radiation spectrum, and enhance the transmissivity by several orders at frequencies close to the resonances.[13–15] Based on this principle, near-field radiative heat transfer has been widely studied and applied to near-field TPV system designs,[17, 21, 23, 28, 32] and recently to TR device designs.[27, 29]

For a given material, the dispersion of its dielectric function, which determines the surface resonant mode, is an intrinsic property. Insulating materials with dielectric function described by a Lorentz model support surface phonon polaritons; metallic materials with dielectric function described by a Drude model support surface plamson polaritons. In order to maximize the radiative transfer, the resonant mode needs to be close to the bandgap frequency ω_g. However, the surface resonant frequencies of natural materials, especially the SPP mode frequency supported by metallic materials, are often much higher than the small ω_g of cells used for thermoradiative power conversion.

We show that nanostructured materials can support additional surface resonances that are closer to ω_g, and, when placed close to the TR cell, can enhance the near-field coupling and the radiative transfer. Therefore the energy conversion can be done more rapidly, and higher power density can be achieved with the same TR cell.

For the following calculations, we use a TR cell with bandgap energy $E_g = 0.3$ eV, which corresponds to the bandgap of InAs.[33] The dielectric function of the TR cell is governed by the direct valence-to-conduction interband transition,[34, 35] and is described by $\epsilon_{cell}(\omega) = \epsilon_r(\omega) + i\epsilon_i(\omega)$. For metallic heat sink, the dielectric function is approximated by the Drude model: $\epsilon_m = 1 - \frac{\omega_p^2}{\omega^2 + i\gamma\omega}$, where ω_p is the plama frequency, γ is the damping rate, and the surface resonant frequency is given by $\omega_0 = \omega_p/\sqrt{2}$. The parameters will be given in the following calculations for each configuration.

The transmissivity and radiative transfer of a TPV or TR system (as shown in Fig. 1) involves grating structures can be calculated based on the scattering theory[36, 37] in combination with the rigorous coupled-wave analysis (RCWA) method.[38, 39] Assume the structure is periodic along x-direction with peridicity p, infinitely long in y-direction, and the TR cell and the grating has a distance d in z-direction, the frequency-dependent transmissivity $\varepsilon_{c,a}(\omega)$ is obtained by integrating wavevector-dependent components $\varepsilon_{c,a}(\omega, k_x, k_y)$ over wavevectors in the x-direction (k_x) and y-direction (k_y), with the integration limit on k_x restricted to the first Brillouin zone due to the periodicity.

$$\varepsilon_{c,a}(\omega) = \frac{1}{2\pi^2} \int_{-\infty}^{\infty} \int_{-\pi/p}^{\pi/p} \varepsilon_{c,a}(\omega, k_x, k_y) dk_x dk_y \tag{3}$$

The wavevector-dependent transmissivity components $\varepsilon_{c,a}(\omega, k_x, k_y)$ can be formulated with scattering theory,[38] and the required scattering matrix between the TR cell and the heat sink is obtained via RCWA calculation.[38, 39] For the transmissivity calculation, the process is the same for TPV and TR systems since temperature is not involved in the optical analysis.

4. RESULTS AND DISCUSSION

We consider a near-field coupled TR system with a metallic heat sink. ZrC has a surface plasmon resonance frequency ω_0 at 0.6 eV,[28, 40] which is about 2 times of the frequency corresponding to the bangap ω_g. We first consider a planar system with a gap of $d = 10$ nm between the TR cell and the ZrC heat sink, as shown in Fig. 1(a). The transmissivity spectrum is calculated and plotted as the blue curve in Fig. 2(a). As expected, a sharp peak is observed at 2 times of ω_g. As a reference, the transmissivity of the TR cell to a blackbody is plotted as the dashed black curve in the same figure. It is seen that in the frequency band of interest, the
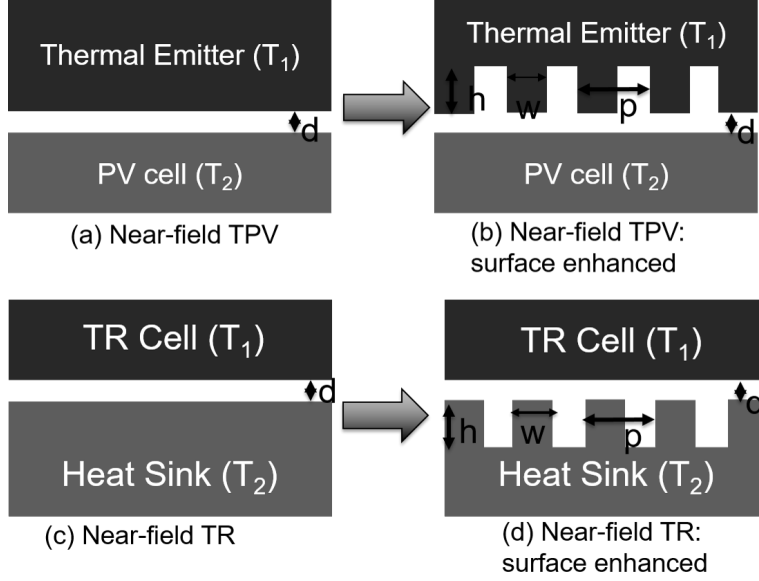
Figure 1. Structures of near-field TPV device (a) with planar thermal emitter, and (b) with periodically structured thermal emitter. Structures of near-field TR device (c) with planar heat sink, and (d) with periodically structured heat sink.

transmissivity due to the near-field coupling to the planar heat sink can indeed exceed the transmissivity to an ideal blackbody. Then we calculate the transmissivity when a grating structure is added to the surface of the heat sink, as shown in Fig. 1(b). The geometrical parameters for the gratings are $h = 60$ nm, $w = 30$ nm, and $p = 60$ nm. The result is shown in the red curve in Fig. 2(a), where multiple resonance peaks are observed. Due to the periodicity, the SPP mode on the metal surface is truncated and folded into multiple bands within the Brillouin zone, and the peaks in the transmissivity spectrum correspond to different order of modes. This can be verified with mode profiles, which are obtained from COMSOL eigenmode solver, and shown in Fig. 2 with three different resonant modes.

Next we calculate the generated power density and efficiency of the TR cell based on equations 1 and 2. When the temperature of the TR cell is at $T_c = 1000$ K, and the heat sink is maintained at $T_a = 300$ K, the power density and efficiency of systems with a blackbody heat sink, the near-field coupled planar heat sink, and the near-field coupled grating heat sink are plotted in Fig. 3(a) and (b). For the planar case, the maximum power density is 3.07×10^4 W/m^2 grating heat sink, the maximum power density is 5.68×10^4 W/m^2, 26.5 times higher than the blackbody heat sink, and 1.8 times higher than the planar heat sink. The maximum achievable efficiency is all above 60%, which is close to the Carnot efficiency of 70% (calculated by $[1-T_a/T_c]$). As mentioned by previous analysis,[24, 29] the chemical potential for maximum power density and maximum efficiency are very different. As we can see from the figure, the power output at maximum efficiency point is very little. So the maximum power density is a better merit to evaluate the performance of the TR cell. When the temperature of the TR cell is at a lower $T_c = 500$ K, while the heat sink is still maintained at $T_a = 300$ K, the power density and efficiency are calculated similarly and plotted in Fig. 3(c) and (d). The peak efficiency is again close to the Carnot efficiency, which is now 40%. The peak generated power density is 13.0, 80.8, and 258.7 W/m^2, for the case of blackbody, planar, and grating heat sink, respectively. Due to the much lower source temperature, the generated power density is two orders lower than the system at $T_c = 1000$ K. However, the near-field coupled heat sink with grating has a more significant enhancement of output power density, at 3.2 times higher than the planar structure.

Note that in the above calculation, we assumed the TR cell to be ideal, where radiative energy can only be extracted from electron-hole pair generation. Non-radiative loss mechanisms, such as Auger and surface defect processes, were not included in the model. On the one hand, including the loss terms will reduce the expected output power; on the other hand, these processes have similar impact on the systems operating at the same
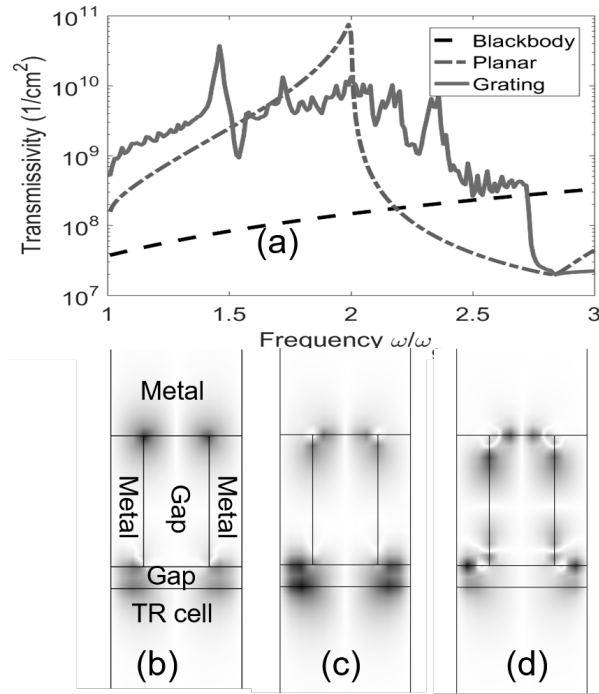
Figure 2. (a) Calculated transmissivity as a function of frequency for three systems: TR cell with ideal blackbody heat sink, TR cell coupled with planar metallic heat sink, TR cell coupled with metallic grating heat sink. The metal is ZrC, with properties and grating geometries described in the main text. (b), (c), and (d) are magnetic field distribution of resonant modes supported by the system.
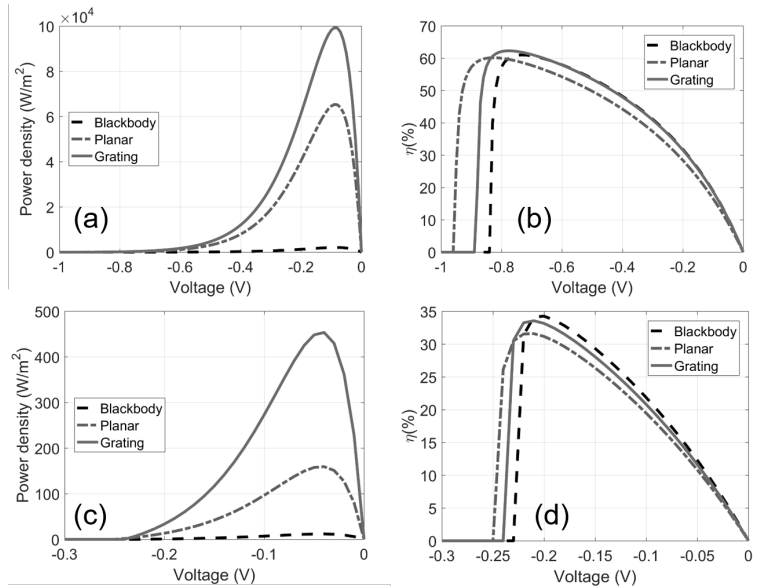

Figure 3. The calculated (a) power density and (b) efficiency for the three systems corresponds to Fig. 2 when the cell is at $T_c = 1000$ K, and the heat sink is at $T_a = 300$ K. The (c) power density and (d) efficiency for the three systems are also shown when the cell is at $T_c = 500$ K, and the heat sink is at $T_a = 300$ K.

temperature, regardless of the heat sink design. Therefore although the absolute numbers of power density will be smaller, the ratio of output power between different heat sink designs will be about the same.[27]

5. CONCLUSIONS

In conclusion, we examined how the nanostructure on the heat sink can increase the TR performance. The performance of the TR can be greatly enhanced with near-field coupling, which occurs by placing a heat sink in close proximity with the cell. Heat sinks supporting surface resonant modes that are close in energy to the bandgap energy of the TR cell are able to boost the radiative transfer of photons and eventually the electric power generation. Metals are good candidates for heat sink of a TR device. However, most metallic materials have surface resonant frequencies much higher in energy than the TR cell bandgap. The mismatch can be addressed with nanostructured surfaces. We show that grating structures support additional surface modes such as truncated surface plasmons and cavity modes depending on the material and geometry. With these tools, we are able to overcome the mismatch in energy of surface resonance and the TR cell bandgap, and design TPV and TR devices for better heat dissipation and enhanced power generation.

REFERENCES

[1] Basu, S., Zhang, Z. M., and Fu, C. J., "Review of near-field thermal radiation and its application to energy conversion," *International Journal of Energy Research* **33**(13), 1203–1232 (2009).

[2] Nefedov, I. S. and Simovski, C. R., "Giant radiation heat transfer through micron gaps," *Phys. Rev. B* **84**, 195459 (Nov 2011).

[3] Guha, B., Otey, C., Poitras, C. B., Fan, S., and Lipson, M., "Near-field radiative cooling of nanostructures," *Nano Letters* **12**(9), 4546–4550 (2012). PMID: 22891815.

[4] Würfel, P. and Würfel, U., [*Physics of Solar Cells: From Basic Principles to Advanced Concepts*], Physics textbook, Wiley (2009).

[5] [*Thermophotovoltaics - Basic Principles and Critical Aspects of | Thomas Bauer | Springer*].

[6] Ferrari, C., Melino, F., Pinelli, M., Spina, P., and Venturini, M., "Overview and status of thermophotovoltaic systems," *Energy Procedia* **45**, 160 – 169 (2014). {ATI} 2013 - 68th Conference of the Italian Thermal Machines Engineering Association.

[7] Park, J., Lee, S., Wu, H., and Kwon, O., "Thermophotovoltaic power conversion from a heat-recirculating micro-emitter," *International Journal of Heat and Mass Transfer* **55**(1718), 4878 – 4885 (2012).

[8] Davies, P. and Luque, A., "Solar thermophotovoltaics: brief review and a new look," *Solar Energy Materials and Solar Cells* **33**(1), 11 – 22 (1994).

[9] Ungaro, C., Gray, S. K., and Gupta, M. C., "Solar thermophotovoltaic system using nanostructures," *Opt. Express* **23**, A1149–A1156 (Sep 2015).

[10] Tuley, R. S. and Nicholas, R. J., "Band gap dependent thermophotovoltaic device performance using the ingaas and ingaasp material system," *Journal of Applied Physics* **108**(8), 084516 (2010).

[11] Chia, L. C. and Feng, B., "The development of a micropower (micro-thermophotovoltaic) device," *Journal of Power Sources* **165**(1), 455 – 480 (2007).

[12] Polder, D. and Van Hove, M., "Theory of radiative heat transfer between closely spaced bodies," *Phys. Rev. B* **4**, 3303–3314 (Nov 1971).

[13] Narayanaswamy, A. and Chen, G., "Surface modes for near field thermophotovoltaics," *Applied Physics Letters* **82**(20), 3544–3546 (2003).

[14] Joulain, K., Mulet, J.-P., Marquier, F., Carminati, R., and Greffet, J.-J., "Surface electromagnetic waves thermally excited: Radiative heat transfer, coherence properties and casimir forces revisited in the near field," *Surface Science Reports* **57**(34), 59 – 112 (2005).

[15] Rousseau, E., Siria, A., Jourdan, G., Volz, S., Comin, F., Chevrier, J., and Greffet, J.-J., "Radiative heat transfer at the nanoscale," *Nat Photon* **3**, 514–517 (Sep 2009).

[16] Laroche, M., Carminati, R., and Greffet, J.-J., "Near-field thermophotovoltaic energy conversion," *Journal of Applied Physics* **100**(6), 063704 (2006).

[17] Ilic, O., Jablan, M., Joannopoulos, J. D., Celanovic, I., and Soljačić, M., "Overcoming the black body limit in plasmonic and graphene near-field thermophotovoltaic systems," *Opt. Express* **20**, A366–A384 (May 2012).

[18] Messina, R. and Ben-Abdallah, P., "Graphene-based photovoltaic cells for near-field thermal energy conversion," **3**, 1383.

[19] Park, K., Basu, S., King, W., and Zhang, Z., "Performance analysis of near-field thermophotovoltaic devices considering absorption distribution," *Journal of Quantitative Spectroscopy and Radiative Transfer* **109**(2), 305 – 316 (2008). The Fifth International Symposium on Radiative Transfer.

[20] Molesky, S. and Jacob, Z., "Ideal near-field thermophotovoltaic cells," *Phys. Rev. B* **91**, 205435 (May 2015).

[21] Liu, X., Wang, L., and Zhang, Z. M., "Near-field thermal radiation: Recent progress and outlook," *Nanoscale and Microscale Thermophysical Engineering* **19**(2), 98–126 (2015).

[22] Elzouka, M. and Ndao, S., "Towards a near-field concentrated solar thermophotovoltaic microsystem: Part i modeling," *Solar Energy* , – (2015).

[23] Jin, S., Lim, M., Lee, S. S., and Lee, B. J., "Hyperbolic metamaterial-based near-field thermophotovoltaic system for hundreds of nanometer vacuum gap," *Opt. Express* **24**, A635–A649 (Mar 2016).

[24] Strandberg, R., "Theoretical efficiency limits for thermoradiative energy conversion," *Journal of Applied Physics* **117**(5), 055105 (2015).

[25] Strandberg, R., "Heat to electricity conversion by cold carrier emissive energy harvesters," *Journal of Applied Physics* **118**(21), 215102 (2015).

[26] Santhanam, P. and Fan, S., "Thermal-to-electrical energy conversion by diodes under negative illumination," *Phys. Rev. B* **93**, 161410 (Apr 2016).

[27] Hsu, W.-C., Tong, J. K., Liao, B., Huang, Y., Boriskina, S. V., and Chen, G., "Entropic and near-field improvements of thermoradiative cells," *Scientific Reports* **6**, 34837 EP – (Oct 2016). Article.

[28] Karalis, A. and Joannopoulos, J., ""squeezing" near-field thermal emission for ultra-efficient high-power thermophotovoltaic conversion," *Scientific Reports* **6**, 28472 (- 2016/07/01/online).

[29] Lin, C., Wang, B., Teo, K. H., and Zhang, Z., "Near-field enhancement of thermoradiative devices," *under review* (2017).

[30] Johnson, P. B. and Christy, R. W., "Optical constants of the noble metals," *Phys. Rev. B* **6**, 4370–4379 (Dec 1972).

[31] Davids, P. S., Intravaia, F., and Dalvit, D., "Spoof polariton enhanced modal density of states in planar nanostructured metallic cavities," *Opt. Express* **22**, 12424–12437 (May 2014).

[32] Liu, X. and Zhang, Z., "Near-field thermal radiation between metasurfaces," *ACS Photonics* **2**(9), 1320–1326 (2015).

[33] Adachi, S., "Optical dispersion relations for gap, gaas, gasb, inp, inas, insb, alxga1xas, and in1xgaxasyp1y," *Journal of Applied Physics* **66**(12), 6030–6040 (1989).

[34] Aspnes, D. E. and Studna, A. A., "Dielectric functions and optical parameters of si, ge, gap, gaas, gasb, inp, inas, and insb from 1.5 to 6.0 ev," *Phys. Rev. B* **27**, 985–1009 (Jan 1983).

[35] Adachi, S., "Model dielectric constants of gap, gaas, gasb, inp, inas, and insb," *Phys. Rev. B* **35**, 7454–7463 (May 1987).

[36] Lussange, J., Guérout, R., Rosa, F. S. S., Greffet, J.-J., Lambrecht, A., and Reynaud, S., "Radiative heat transfer between two dielectric nanogratings in the scattering approach," *Phys. Rev. B* **86**, 085432 (Aug 2012).

[37] Liu, X. L. and Zhang, Z. M., "Graphene-assisted near-field radiative heat transfer between corrugated polar materials," *Applied Physics Letters* **104**(25), 251911 (2014).

[38] Moharam, M. G., Gaylord, T. K., Grann, E. B., and Pommet, D. A., "Formulation for stable and efficient implementation of the rigorous coupled-wave analysis of binary gratings," *J. Opt. Soc. Am. A* **12**, 1068–1076 (May 1995).

[39] Li, L., "Use of fourier series in the analysis of discontinuous periodic structures," *J. Opt. Soc. Am. A* **13**, 1870–1876 (Sep 1996).

[40] Modine, F. A., Haywood, T. W., and Allison, C. Y., "Optical and electrical properties of single-crystalline zirconium carbide," *Phys. Rev. B* **32**, 7743–7747 (Dec 1985).